A SIMPLE POLARIZED-BASED DIFFUSED REFLECTANCE COLOUR IMAGING SYSTEM

H. H. E. Jayaweera[1], B. Anderson[2] and M.J. Eghan[2]
[1]Centre for Instrument Development, Department of Physics, University of Colombo, Sri Lanka
[2]LAFOC, Department of Physics, University of Cape Coast, Cape Coast, Ghana

ABSTRACT
A simple polarized-based diffuse reflectance imaging system has been developed. The system is designed for both in vivo and in vitro imaging of agricultural specimen in the visible region. The system uses a commercial web camera and a halogen lamp that makes it relatively simple and less expensive for diagnostic research and teaching. The system has been used to demonstrate the difference between a yellow colour of a diseased cassava leaf and that of a senescence cassava leaf qualitatively using diffused reflectance images. Predicting the area of the sample using a method of counting dark pixels is presented. This method avoids complex and more computational power required by edge detection algorithms. The performance of the suggested method can be seen for 50 samples of leaves. This suggest that polarized diffused reflectance image lends itself to extraction of physical information.

INTRODUCTION

Among various diagnostic optical techniques, reflectance spectroscopy is considered to be one of the powerful techniques in a large variety of non-destructive, non-intrusive, fast and real-time applications in many fields, such as agriculture, medicine and environmental monitoring (Curran *et al.,* 1992; Batten, 1998; Cheng and Boas,1998; Foley *et al.,* 1998; Young-Ah *et al.,* 1999; Cozzolino *et al.,* 2001; Ji *et. al.,* 2002; Cozzolino and Moron , 2003; Qin and Lu, 2008; Zhu *et al.,* 2006; Stelzle *et al.,* 2010; Stelzle *et al.,* 2011). The ability of reflectance technique to be used in the mentioned fields is critically useful, because there is no or little sample preparation, which in effect reduces human error, time and cost.

Most material surfaces act like a dielectric boundary such that the surfaces scatter and absorb light (Born and Wolf, 1965). The scattering may result from specular and/or diffuse reflection. The specular component is a surface phenomenon, where the Snell's laws are obeyed and contains' information about the surface topology, such as texture. For uneven surfaces the specular components are concentrated in a compact lobe in the vicinity of the specular direction. This concentration of light intensity causes highlights in bright image scenes. These strong highlights cause problems for intensity related analysis thus producing erroneous results (Nayar *et al.,* 1993; Bhat and Nayar, 1995). So these specularities are often eliminated in image processing, when physical

and chemical information of the material is required.

The diffuse reflection results when light penetrates through a surface and undergoes multiple scattering and re-emerges at the surface from the medium. The back-scattered light is distributed in a wide range of directions within the medium, thus becoming depolarised relative to the incident light, giving an image a dull appearance (Nayar *et al.,* 1993). The spectral dimensions of diffuse reflection are generally governed by the molecular makeup of the material medium, and so much of the physical and chemical information about a material can be obtained from the diffuse reflected part of the reflection.

For both synthetic and natural materials, diffuse reflection spectroscopy has been used, in both basic and applied research, for quantitative and qualitative analysis of various materials, (Kienle *et al.,* 1996; Doornbos *et al.,* 1999; Ji *et al.,* 2002; Fabbri *et al.,* 2003; Dean *et al.,* 2008; Yu *et al.,* 2008; Stelzle *et al.,* 2010; Stelzle *et al.,* 2011). In biological and medical research, the study of respiratory enzymes in vivo has become possible due to diffused reflectance. Amount of glucose and quantification of tissue absorption and scattering in vivo can be researched into using diffused reflectance (Cameron and Li, 2007; Yu *et al.,* 2008)

Also, polarized light-matter interactions has made polarized-based optical techniques to have potential applications (MacKintosh *et al.,* 1989; Schmitt *et al.,* 1992; Jacques *et al.,* 2000; Ramella-Roman *et al.,* 2002; Arimoto, 2007; O'Doherty *et al.,* 2007; Cameron and Li, 2007; Stelzle *et al.,* 2011). Polarimetric dimensions are governed by sample geometry and surface properties and can vary substantially with viewing geometry, but spatial and spectral signatures, are reasonably stable with viewing geometry. However, the advantages of polarizationare that polarized light reduces the degrees of freedom of the reflected lights and eliminates the polarization memory of specular reflected light (MacKintosh *et al.,* 1989), when cross polarizers are used. Specular reflection can be eliminated, when information about the surface properties and image acquisition geometry are not required. Whereas polarimetric signatures present an attractive prospect for increasing the dimension of sensed data, they also present new collection, modelling, and analysis challenges. The depth of penetration of a polarized light depends strongly on the optical properties of the medium at each present wavelength (Liu *et al.,* 2005).

Most of the polarized-based reflectance imaging systems described in literature (MacKintosh *et al.,* 1989, Liu *et al.,* 2005) employ specialized equipment that is not easily accessible to most researchers. With the advancement in technology, commercial web camera (web-cam), which are fast, cheap but reliable imaging systems and making use of cheap Complementary Metal Oxide Semiconductor (CMOS) are now available.

In this study, we present a low cost and simple polarized-based diffuse reflectance imaging system (PBDRIS) that uses a web-cam. The relevance of this instrument to measure diffuse reflectance is illustrated with infected African cassava mosaic diseased leaves and non-infected cassava leaves.

MATERIALS AND METHODS

The general arrangement for our polarized-based diffused reflectance colour imaging system is illustrated in Figure 1.A photograph of the complete instrumentation is shown in Figure. 2.Light source for diffused reflection is a30 W halogen lamp housed in cooling vents that allow convection currents to bathe the lamp with cooler air during operation.

The entire system is housed in a wooden frame which was designed by us and built by the University carpentry division (Figure 2a). A well dried red wood of dimension 1.5 x 1.5 cm was used to form the wooden frame of 12 x 12 x 21 cm as the outer dimensions. The actual sample chamber, rectangular in shape, 9 x 9 x 12.5 cm was enclosed with a black card-board as well as its floor. Anupper chamber housed the major electronic components; the web-cam, light

source and its power supply (step-down transformer), and the dimmer (Figure 2b),of the system. The electronic system is controlled by a personal computer (PC, Dell), which is used for data acquisition, storage and image analysis.

The lamp is powered externally by a 12 VDC step-down transformer from the mains (240 V, 50 Hz). Attached to the light is a dimmer that controls the light intensity in relation to the sample. This light intensity is monitored by

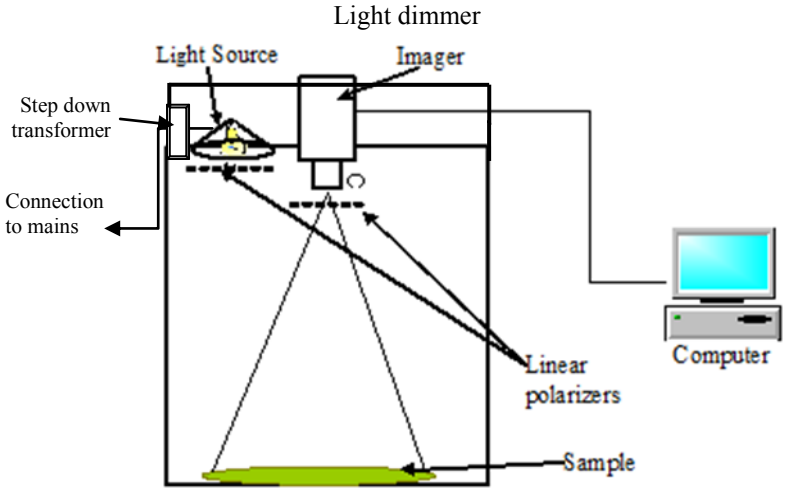

Figure 1: Schematic view of the completed polarized-based multispectral imaging system

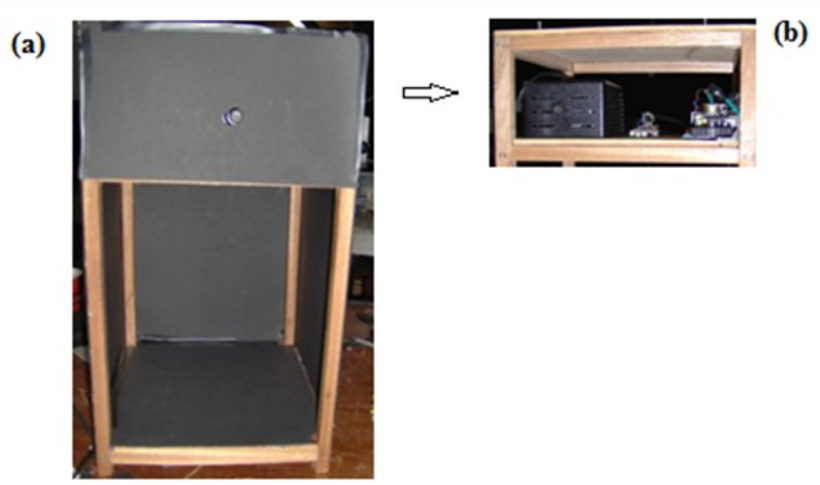

Figure 2: System instrumentation: (a) complete system with the sample chamber (lower) and the upper chamber (fully covered) which holds the electronics. (b) Uncompleted system instrumentation showing the upper chamber which holds the web-cam, light source, step-down transformer and dimmer.

alight intensity histogram, an algorithm that was developed by us using MATLAB software (Matlab 7.10.0, 2010).

A metallic spherical reflector lining the inner part of the lamp-house assists to direct the greatest possible level of luminous flux into the collector lens system for delivery unto the sample. The lamp's position in relation to the spherical reflector and collector optical axis can be adjusted using a translating screw. The spectral range of the light source is from 400 nm to about 900 nm. Figure 3 shows the emission spectrum of the light source as was measured with an Ocean Optics USB 4000 Spectrometer.The spectra broadness of the light source makes it appropriate for reflection imaging.

A commercial web camera (web-cam) with USB 2.0 (Universal Serial Bus) interface is used as the colour (Red, Green and Blue) imager. The web-cam has 640 × 480 (307,200 pixels = 0.3 Mega pixels) absolute maximum resolution and each Red, Green and Blue channel has 8 bit intensity depth. The size of the CMOS (Complementary Metal Oxide Semiconductor) sensor of the web-cam is 4.86 mm ×3.64 mm.

The viewing area of the imager has been set to 16 x 12 cm^2. Hence, the system has 1600 pixels per square centimeter pixel density and 10.9 times magnification. The web-cam is capable of acquiring 15 frames per second when it is at its maximum resolution.

Because the system is mainly intended to image diffuse reflection, linear polarizer and analyzer (NT43-781, Edmunds Optics) have been used to eliminate the specular reflection. The linear polarizer was placed in front of the light source and the analyzer placed in front of the imager. The polarizer and analyzer were mounted in such a way that the polarization planes aretotally crossed.

Imaging Procedure

From the PC, our developed MATLAB code was used to control the electronics to aid the data acquisition. The image acquisition process, using the imaging system, is shown as a flow chart (Figure 4).The intensity distribution of the viewing area for a white paper is measured. This spatial domain of the light intensity distribution is used to normalize sample images in order to compensate for the error due to uneven light distribution from the source. When the background image is subtracted from sample image, features of the sample can be easily extracted.

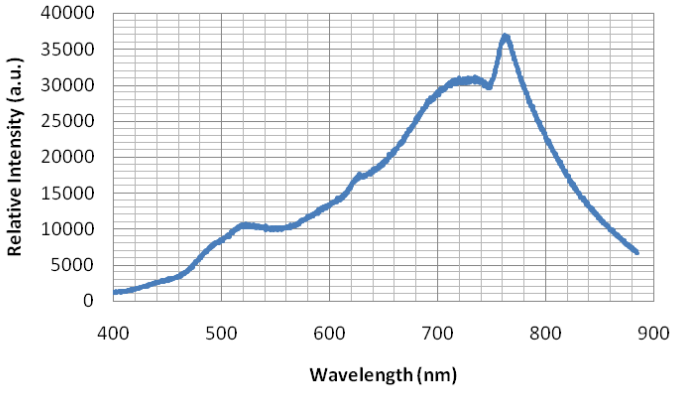

Figure 3: Emission spectrum of the light source in the system: measured using Ocean Optics USB 4000 Spectrometer.

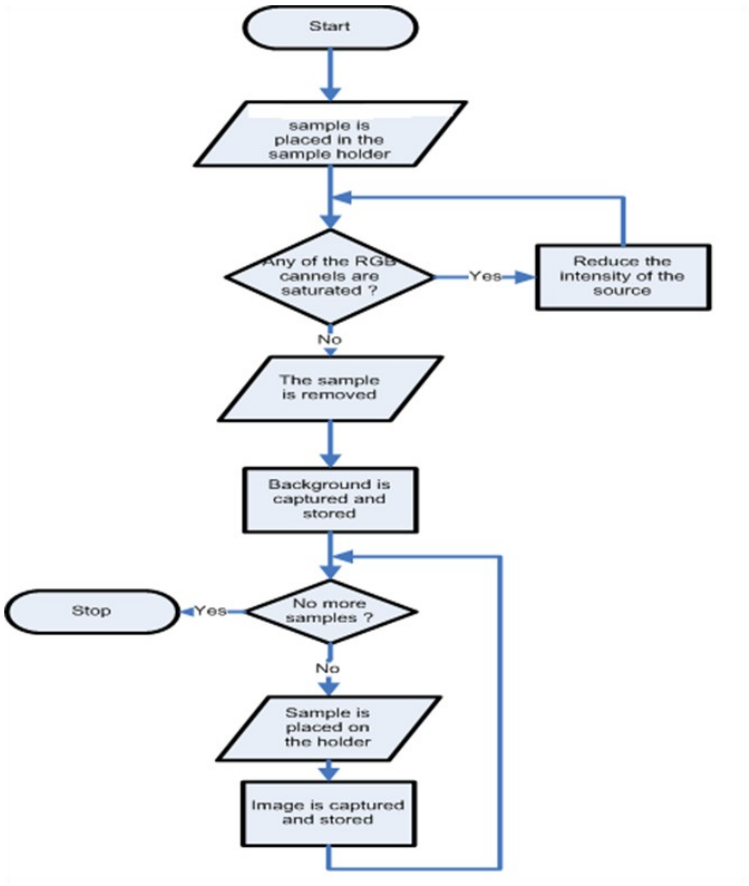

Figure 4: Flow chart of image acquisition process

In the event that many samples of different areas are to be compared, other than the correction of the uneven distribution of the light intensity, effect due to the area should be corrected. In order to eliminate the area dependence an edge detection algorithm was used to calculate the area of the samples. The method of counting dark pixels and predicting the area of the sample was studied. In this suggested method, background subtracted image is considered.

The total number of zero intensity (dark) pixels was subtracted from the total number of pixels and that number is a good estimate for the area of the sample. Our developed imaging system was also used to image severely infected African mosaic diseased cassava (ACMD) leaf, mildly infected, a healthy cassava leaf (control) and a senescence cassava leaf.

RESULTS

The intensity distribution of the viewing area for a white paper measured is shown in Figure 5. The positions of the light source and the camera are marked in the figure. From Figure 5, the normalized intensity of the top graph, which is depicting the horizontal cross-section of the image plane taken from left to right decreases.

This shows the brightest position of the light source in the imaging plane. Likewise, the left graph, depicts the normalize intensity along the

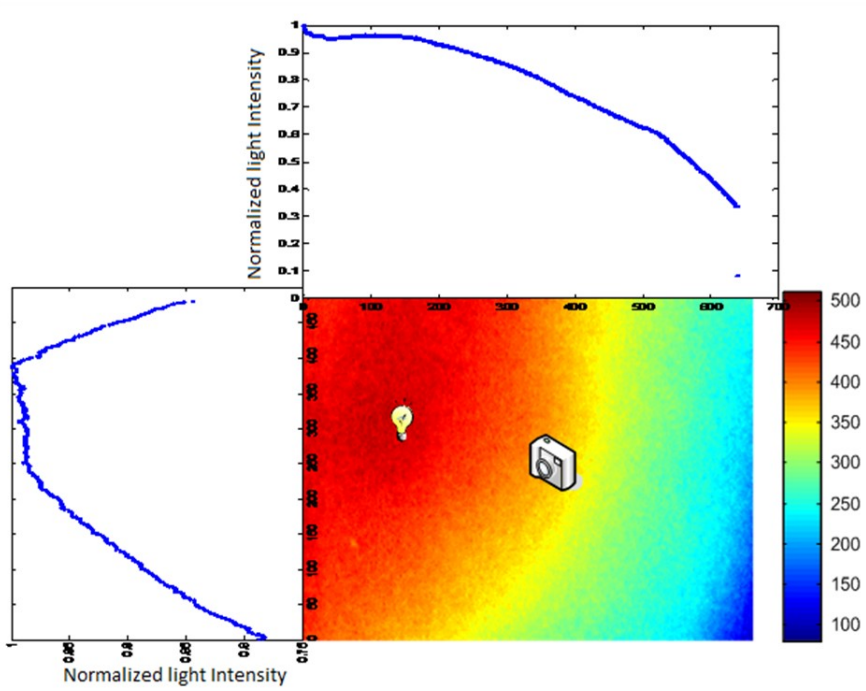

Figure 5: Light intensity distribution through the viewing area.

vertical cross-section of the image plane. Both graphs indicate non-uniformity of the light source in the image plane.

The method of counting dark pixels and predicting the area of the sample yielded a good estimate for the area of the sample. Hence, by using this method, complex and more computational power that consume edge detection algorithms was avoided. The performance of the suggested method can be seen for 50 samples of leaves in Figure 6.

Figure 7 shows the images of classes of healthy and diseased leaves imaged with the system. The classes of the cassava leaves are made up of healthy green, mildly mosaic infected, severely mosaic infected and healthy senescence cassava leaf.

Figure 8 shows an example of how the images of the cassava leaves were acquired and processed using the image acquisition processes in the flow chart. Figure 8A shows the background image (A) of the system while figure 8B shows cassava leaf sample with the background (B). The image in (A) was subtracted from image in (B) to get the image of the cassava leaf (C). When the edge algorithm was applied to image (C), image (D) was obtained.

The image in (C) does not show any concentration of highlight intensities (specular component) on the leaf surface. Figure 9 shows the pixel histogram of the Red (R), Green (G) and Blue (B) colours from each of the leaves in Figure 7. There are significant differences in the R-, B- and G-pixel spectra of all the leaves implying the leaves are different and this qualitative information lends itself to discrimination algorithms using RGB. The Senescence leaf showed a very unique RGB pixel histogram depicting high pixel intensities for R and G and broader one for B. This could be attributed to the yellowish colour as yellow is a combination of Red and Green. This means that though the leaf appears yellowish to the human eye there is

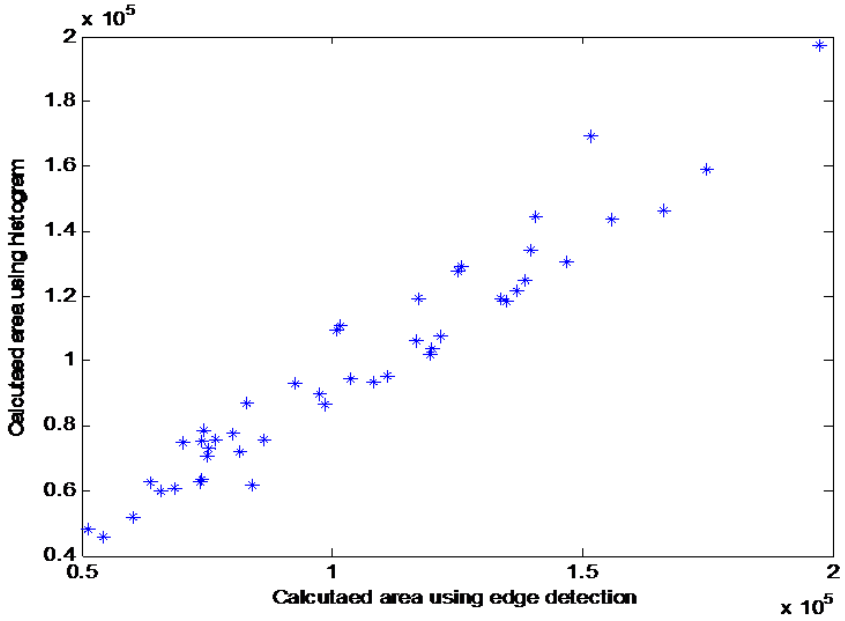

Figure 6: Correlation of area calculation using edge detected technique and histogram technique

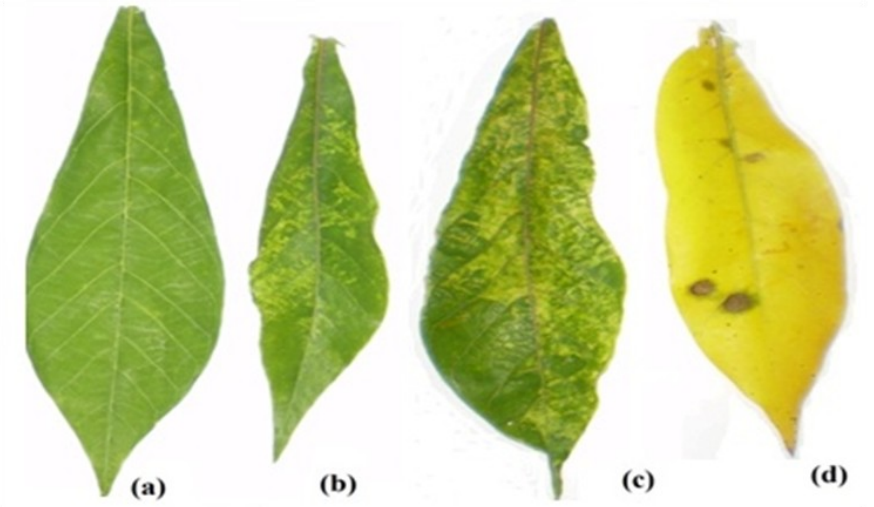

Figure 7: Images of cassava leaves: (a) is the healthy green cassava leaf, (b) is the mildly infected mosaic cassava leaf, (c) is the severely infected mosaic cassava leaf and (d) a senescence cassava leaf.

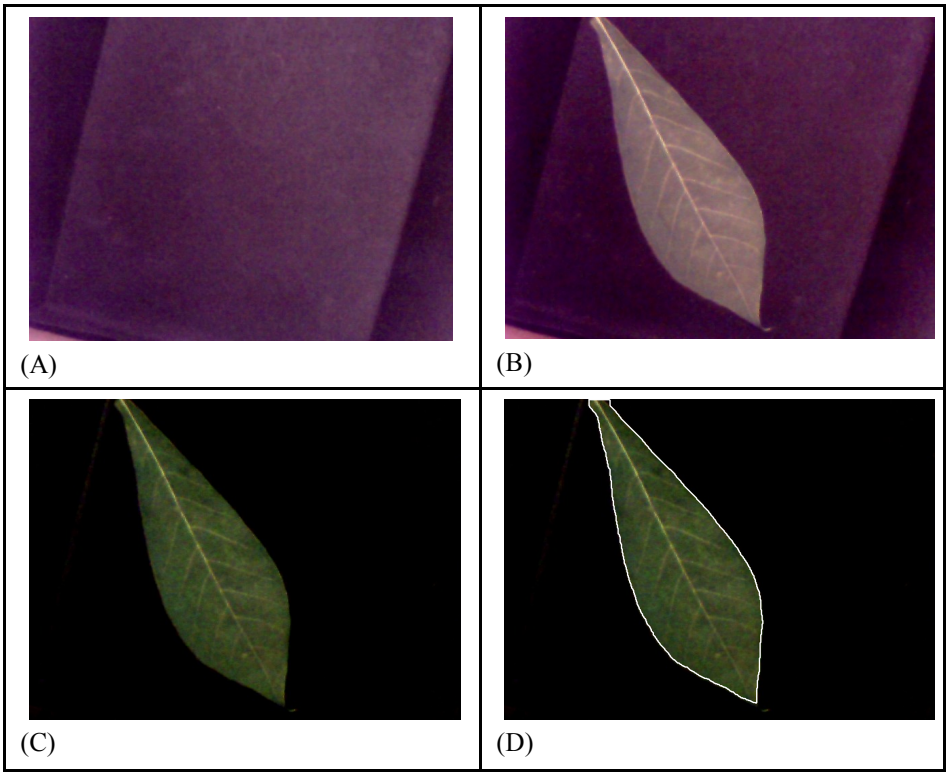

Figure 8: Example of image acquisition processes for cassava leaf: A – Background image; B - image of the cassava leaf with the background ; C - Processed Image:- Background image (A) subtracted from image in (B); D - Edge detected image of image (C).

a sizable amount of B in it. On the effect of the ACMD on the leaves we could see that due to the severity of the ACMD on the leaf (b) the G-pixel histogram shift is broader than most of the other G-pixel histograms. Also the frequency of the pixels (pixel counts) reduced compared to that of the healthy and mildly affected leaves. From the RGB-pixel histograms, the level of the effect of the disease lend itself to easy quantification using our developed matlab codes on the captured images by the system (see Figure 8).

DISCUSSION

A simple polarized-based diffuse reflectance imaging system, made up mainly of halogen lamp, web camera, which is relatively cheap, and linear polarizers has been built and demonstrated. The sample images acquired did not show any concentrated lube of highlight intensities (specular component) on the leaf surface, which normally produces erroneous images. Thus, there was no need for vision algorithms for scene segmentation. The cassava mosaic disease diagnostics demonstrated, provided valuable information about the status of the infected and uninfected leaf samples. The RGB spectral showed the difference between a diseased cassava leaves and that of a senescence cassava leaf.

Ghana, an agricultural based country, has many biological samples such as orange, watermelon, banana and pawpaw and they all have diseased

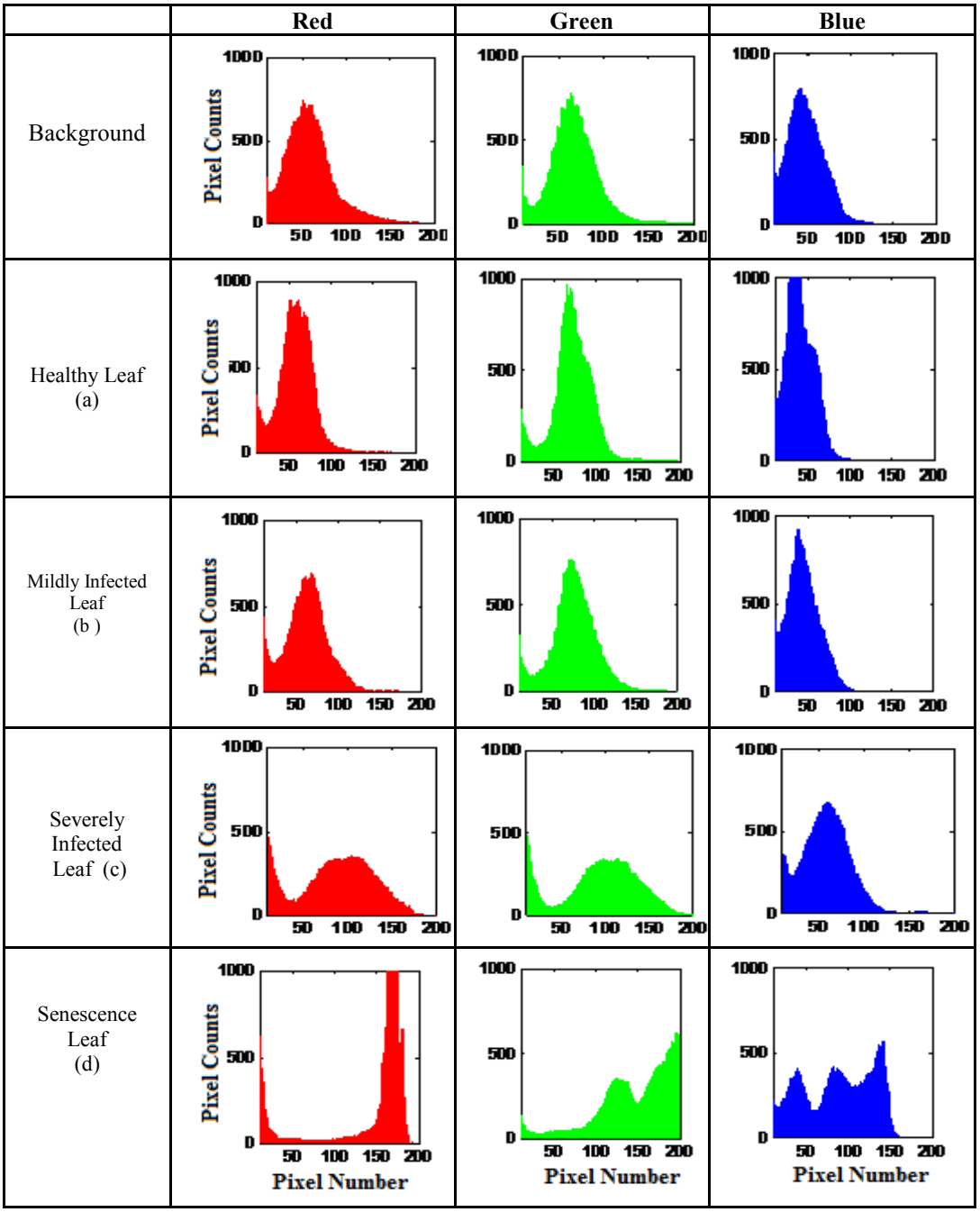

Figure 9: RGB-pixel histogram of various leaves in figure 7: a) background, b) severely infected CMD leaf c) healthy cassava leaf, d) mildly infected CMD leaf and d) senescence cassava leaf image

related problems with their leaves, for which this system can be used as are search tool.
The web-cam can readily be replaced with an advance web-cam that can record other wavelengths with corresponding light source. The light source in the present system is somewhat not evenly distributed, leading to image correction. However, an evenly distributed light source can be used.

Using other analytic techniques, such as multivariate image analysis (Gonzalez *et al.,* 2004; Esbensen *et al.,* 1994) this system can be used for application in medical and biological diagnostics as well as in food science where detection of complex samples is required for quantification using imaging.

While this system is not yet a replacement for sophisticated imagers, it is an attractive tool due to its simplicity, versatility, and low cost. In general, this imager can be a valuable tool for teaching and research in applied optics.

ACKNOWLEDGMENTS

Assistance from the International Science Programs (ISP) of the Uppsala University, Sweden and Atomic and Molecular Spectroscopy Group of the Lund University is greatly acknowledged. Hiran H E Jayaweera is grateful to ISP for funding his stay at Lafoc-UCC. Anderson and Eghan are also grateful to the Abdus Salam International Center for Theoretical Physics (ICTP) for their financial support during their stay at the ICTP as regular associates.

REFERENCES

Arimoto, H. (2007). Estimation of water content distribution in the skin using dual band polarization imaging, *Skin. Res. Tech.* 13: 49-54.

Batten, G. D. (1998). Plant analysis using near infrared reflectance spectroscopy: the potential and the limitations. *Australian Journal of Experimental Agriculture* 38(7): 697 -706.

Bhat, D.N. and Nayar, S.K. (1995). Stereo in the presence of specular reflection, IEEE International Conference on Computer Vision,http://doi.ieeecomputersociety.org/10/1109/ICCV.1995.466813

Born, M. and Wolf, E. (1965). Principles of Optics, London: Pergamon.

Cameron, B. D. and Li, Y. (2007). Polarization-based diffuse reflectance imaging for non invasive measurements of glucose. *J. of Diabetes Sci. and Technology*.1(6): 873-878.

Cheng, X. and Boas, D. A. (1998). Diffuse optical reflection tomography with continuous-wave illumination. *Optics Express* 3 (3): 118-123.

Cozzolino, D, and Moron, A. (2003). The potential of near-infrared reflectance spectroscopy to analyse soil chemical and physical characteristics. *J. of Agricultural Sc.*140: 65-71.

Cozzolino, D., Fassio, A. and Gimenez, A. (2001). The use of near-infrared reflectance spectroscopy (NIRS) to predict the composition of whole maize plants. *Journal of the Science of Food and Agriculture* 81(1): 142-146.

Curran, P. J., Dungan, J. L., Macler, B. A., Plummer, S. E. and Peterson, D. L. (1992). Reflectance spectroscopy of fresh whole leaves for the estimation of chemical concentration. *Remote Sensing of Environment* 39(2): 153-166.

Dean, P., Shaukat, M. U., Khanna, S. P., Chakraborty, S., Lachab, M., Burnett, A., Davies, G. and Linfield, E. H. (2008). Absorption-sensitive diffuse reflection imaging of concealed Powders using a terahertz quantum cascade laser. *Optics Express* 16 (9): 5997-6007.

Doornbos, R. M. P., R. Lang, M. C. Aalders, F. W. Cross, and H. J. C. M. Sterenborg. (1999). The determination of in vivo human tissue optical properties and absolute chromophore concentrations using spatially resolved steady-state diffuse reflec-

tance spectroscopy. *Physics in Medicine and Biology* 44(4): 967-981.

Esbensen, K., Midtgaard, T., Schonkopf, S., Guyof, D. (1994). Multivariate Analysis - A Training Package, CAMO ASA, Oslo, Norway: Wiley and Sons.

Fabbri, F., Francesschini, M. A. and Fantini, S. (2003). Characterization of spatial and temporal variations is the optical properties of tissue-like media with diffuse reflectance imaging. *Appl. Opt.,* 42(16): 1183-1201.

Foley, W. J., McIlwee, A., Lawler I., Aragones, L., Woolnough, A. P. and Berding, N. (1998). Ecological applications of near infrared reflectance spectroscopy – a tool for rapid, cost effective prediction of the composition of plant and animal tissues and aspects of animal performance. *Oecologia,* 116(3):

Gonzalez, R. C., Woods, R. E. and Eddins, S. L, (2004). Digital Image Processing Using MatLab Prentice Hall, Upper Saddle River, NJ.

Jacques, S. L., Ramella-Roman, J. C. and Lee, K. (2000). Imaging superficial tissues with polarized light, *Lasers Surg. Med.* 26: 119-129.

Ji, J. F., Balsam, W., Chen, J. and Liu, L. W. (2002). Rapid and quantitative measurement of hematite and goethite in the Chinese loess-paleosol sequence by diffuse reflectance spectroscopy. *Clays and Clay Minerals* 50: 208-216.

Kienle, A., L. Lilge, M. S. Patterson, R. Hibst, R. Steiner, and B. C. Wilson, B.C. (1996). Spatially resolved absolute diffuse reflectance measurements for non invasive determination of the12 optical scattering and absorption coefficients of biological tissue. *Appl. Opt.* 35(13):2304-2314.

Liu, Y., Kim Y. Y., Li, X. and Backman, V. (2005). Investigation of depth selectively of polarization gating for tissue characterization. *Applied Optics* 31(11): 601-611.

MacKintosh, F. C., Zhu, J. X., Pine, D. J., and Weitz, D. A. (1989). Polarization memory of multiply scattered light, *Phys. Rev.* B 40: 9342-45.

Matlab, 7.10.0 (2010). R2010a, Mathworks Inc. USA.

Mobley, J. and Vo-Dinh, T. (2003). Biomedical Photonics Handbook, ch. Optical Properties of Tissue. CRC Press LLC, Boca Raton, USA.

Nayar, S. K., Fang, Xi, S. and Terrance, B. (1993). Removal of specularities using color and polarization, *Proc. CVPR '93' IEEE Computer Society Conf. June 15-17*,IEEE. pp 583 -590.

O'Doherty, J., Henricson, J., Anderson, C., Leahy, M. J., Nilsson, G. E. and Sjöberg, F. (2007). Sub epidermal imaging using polarized light spectroscopy for assessment of skin microcirculation, *Skin Res. Tech.*13 (4): 472–484.

Qin, J. and Lu, R. (2008). Measurement of the optical properties of fruits and vegetables using spatially resolved hyperspectral diffuse reflectance imaging technique. *Postharvest Biology and Technology.* 49(3): 355-365.

Ramella-Roman, J. C., Jacques, S. L. and Lee, K. (2002). Imaging skin pathology with polarized Light. *J. Biomed. Opt.* 7: 329-340.

Ramella-Roman, J. C., Lee, K., Prahl, S. A. and Jacques, S. L. (2004). Design, testing, and clinical studies of a handheld polarized light camera, *J. Biomed. Opt*. 9: 1305-1310.

Schmitt, J. M., Gandjbakhche, A. H. And Bonnar, R. F. (1992). Use of polarized light to Discriminate short-pass photons in a multiply scattering medium, *Appl. Opt.* 31: 6535 -6539.

Stelzle, F., Tangermann-Gerk, K., Adler, W., Zam, A., Schmidt, M., Douplik, A., Nkenke, E. (2010). Diffuse reflectance

spectroscopy for optical soft tissue differentiation as remote feedback control for tissue-specific laser surgery. Lasers in Surgery and Med. 42(4): 319– 325.

Stelzle, F., Zam, A., Adler, W., Tangermann-Gerk, K., Douplik, A., Nkenke, E., Schmidt, M. (2011). Optical Nerve Detection by Diffuse Reflectance Spectroscopy for Feedback Controlled Oral and Maxillofacial Laser Surgery. *Journal of Trans. Medicine,* 9: 20.

Young-Ah, W., Hyo-Jin, K. Jung, H.C., Hoeil, C. (1999). Discrimination of herbal medicines according to geographical origin with near infrared reflectance spectroscopy and pattern recognition techniques. *Journal of Pharmaceutical and Biomedical Analysis* 21(2): 407-413.

Yu, B., Lo, J. Y., Kuech, T. F., Palmer, G. M., Bender, J. E., and Ramanujama, N. (2008). Cost-Effective diffuse reflectance spectroscopy device for quantifying tissue absorption and scattering invivo. *J. of Biomedical Optics,* 13(6): 060505-1-3.

Zhu, C., Palmer, G. M., Breslin, T. M., Harter, J. and Ramanujam, N. (2006). Diagnosis of breast cancer using diffuse reflectance spectroscopy: Comparison of a Monte Carlo versus partial least squares analysis based feature extraction technique. *Lasers in Surgery and Medicine.* 38(7): 714-724.